J Therm Anal Calorim (2009) 97:433–436
DOI 10.1007/s10973-009-0086-4

Synthesis and thermal properties of nanoparticles of bioactive glasses containing silver

José Renato J. Delben · Odair M. Pimentel · Marlene B. Coelho · Pollyanna D. Candelorio · Leonardo N. Furini · Fábio Alencar dos Santos · Fábio S. de Vicente · Angela A. S. T. Delben

ICTAC2008 Conference

Abstract Calcium phosphate bioactive glasses (BG) and some ceramics are candidates for implantation due to their excellent bonding to bone. Silver is a bactericidal element and can be easily introduced in glasses and ceramics. In this work, nanometer-sized bioactive glass particles doped with silver were produced and characterized by Thermal Gravimetric analysis (TG), Fourier Transform Infrared Spectroscopy (FTIR), Scanning Electron Microscopy (SEM), and X-ray Diffraction (XRD). Water hygroscopy was reduced with increasing silver content. The increase in the amount of silver caused an increase in quartz and metallic silver crystallization while reducing the BG transformation into hydroxyapatite. It was observed the silver reduction leading to metallic silver formation for bioactive glasses containing high amount of silver.

Keywords Bioactive glasses · Ceramics · FTIR · SEM · TG · XRD

Introduction

Several biomaterials have been developed for medical purposes; a majority of these materials were developed for bone regeneration or replacement due to age-related tissue loss or accident [1]. After implantation into the body, these materials should not produce any adverse response; they must be non-toxic, non-carcinogenic, non-antigenic, and non-mutagenic. Additionally, they also need to exhibit adequate mechanical properties.

Biomaterials can be produced from many kinds of materials, such as synthetic polymers, metals, ceramics, and natural macromolecules that have the proper morphology and properties according to the application requirements. Also, a series of bioactive glasses (BG) has been in development since 1969. These glasses were initially prepared by fusing different oxides, specifically 45% SiO_2, 24.5% CaO, 24.5% NaO_2, and 6% P_2O_5 [2] (patented as 45S5 Bioglass®). These glasses can form a chemical bond with bone tissue and present higher osteoblastic activity than hydroxyapatite. In 1991, Rounan Li et al. obtained BG with a composition of 70% CaO and 30% SiO_2 by the sol–gel method. This new glass system offered a surface with a higher reactivity and a higher degradation rate compared to bioactive glasses obtained by fusion. Chatzistavrou et al. studied the crystallization mechanism and the biological response of the SiO_2–CaO–NaO_2–P_2O_5 system as function of particle size [3].

J. R. J. Delben (✉) · P. D. Candelorio ·
L. N. Furini · F. Alencar dos Santos · F. S. de Vicente ·
A. A. S. T. Delben
Departamento de Física, UFMS, Cidade Universitária, CP 549,
Campo Grande, MS CEP 79070-900, Brazil
e-mail: delbenbr@yahoo.com.br

O. M. Pimentel
Departamento de Patologia, CCBS/UFMS, CP 549, Campo
Grande, MS CEP 79070-900, Brazil

J. R. J. Delben · P. D. Candelorio · F. S. de Vicente ·
A. A. S. T. Delben
DCC-Faculdade de Medicina, UFMS, Cidade Universitária,
CP 549, Campo Grande, MS CEP 79070-900, Brazil

J. R. J. Delben · P. D. Candelorio · F. S. de Vicente ·
A. A. S. T. Delben
Pós-Graduação em Saúde e Desenvolvimento na Região
Centro-Oeste, UFMS, Cidade Universitária, CP 549,
Campo Grande, MS CEP 79070-900, Brazil

M. B. Coelho
EMBRAPA Gado de Corte, CP 549, Campo Grande, MS CEP
79070-900, Brazil

In order to improve the mechanical properties or biological responses, different oxides were added to bioactive glasses, such as zinc oxide, magnesium oxide, zirconia, titania, boron oxide and silver. Zinc oxide improved the mechanical resistance and bone formation in vitro and in vivo. It also improved the ability of the glass to bond to bone, decreased solubility in simulated body fluid (SBF), and increased BG osteoconductivity [4, 5]. Titania is miscible in the vitreous matrix at high temperatures and induces phase separation as the temperature decreases. Titania induced calcium-phosphate crystallization and improved chemical resistance against deionized water from SBF by forming Ti–O–P bonds that are stronger than P–O–P bonds [6–8]. Magnesium oxide was biocompatible and enhanced osteoblastic formation in vitro. It also promoted osteoblastic differentiation [9, 10]. In the 45S5 bioactive glasses, the hydroxyapatite layer had a faster growth rate when B_2O_3 was used instead of SiO_2 [11–13], since B_2O_3 enhanced human mesenchymal cell growth and differentiation. The boron oxide glasses were completely transformed into hydroxyapatite in less than 4 days, while glasses of boron oxide and silica were partially converted into hydroxyapatite after 70 days and still possessed residual silica.

Presently, bioactive glasses containing silver have been developed, because silver is bacteriostatic, bactericidal, and does not damage human cells, which improves the period after surgical implantation [14]. The bactericidal role of bioactive glass is related to high pH, ionic concentration and osmotic pressure (higher than 4% after 60 min with 1.7% of powder/mm of bacteria culture). Due to these biological properties, silver has been added to polyurethane, hydroxyapatite and bioactive glasses. Maria Bellantone et al. [15] and Clupper [16] verified that the silver inclusion did not spoil glass bioactivity.

In the present work, we report the physical properties of bioactive glasses containing silver prepared by the sol–gel method and characterized by thermal gravimetric analysis (TG), Fourier transform infrared spectroscopy (FTIR), scanning electron microscopy (SEM), and X-ray diffraction (XRD). We obtained nanometer-sized particles of bioactive glasses. The silver reduction has previously been reported for silica glasses, we observed the silver reduction resulting in metallic silver for bioactive glasses containing a minimum of 3% silver.

Methods

The sol–gel method was applied in the synthesis of bioactive glasses. The advantages of this method are the low temperatures that are required, the homogeneous distribution of the components, and the possibility of porosity and particle size control [17].

The preparation consisted of the following steps: mixing the precursors, hydrolysis, gelation, aging, drying, and stabilization. The samples were prepared in the $60SiO_2$–$36CaO$–$4P_2O_5$ system with 0, 1, 3 and 5 mol % of silver. Initially, 103.5 mL of deionized water was mixed with 90 mL of ethanol (from ABSynth) and 5.76 mL of nitric acid 2 M and this mixture was stirred for 1 h. Next, 29.7 mL of tetraethoxysilane (TEOS, from Sigma-Aldrich), 3.03 mL of triethyl phosphate (TEP, from Sigma-Aldrich), 21.408 g of calcium phosphate (from Cinética Química), and 0.392 g of silver nitrate (from Merck) were added. After the addition of each compound, the mixture was stirred for 1 h. Finally, ammonium hydroxide was drop wised in the mixture up to the start of gelatinization. After gelatinization, the samples were dried at 130 °C for 24 h (130 °C/24 h) and then treated at 600 °C for 4 h (600 °C/4 h) in air to eliminate organics and form glass nanoparticles. The treatment temperature was chosen above the temperatures required to complete water elimination.

The samples were analyzed by thermogravimetry in a Shimadzu TA-50H thermogravitometer, using a platinum crucible under nitrogen and synthetic dry air. FTIR was performed in a Termo Nicolet spectrometer NEXUS 670, with a resolution of 8.0 cm^{-1}. The morphology was analyzed in a JEOL 6830LV scanning electron microscope (SEM). The crystalline phases were determined by X-ray diffraction (XRD) in a Rigaku–Rotaflex RU200B with CuK radiation, operating at 50 kV and 100 mA. The XRD patterns were analyzed using JSPDS data.

Results and discussion

In TG curves (Fig. 1), the samples treated at 600 °C/4 h showed continuous mass loss until 500 °C. These losses

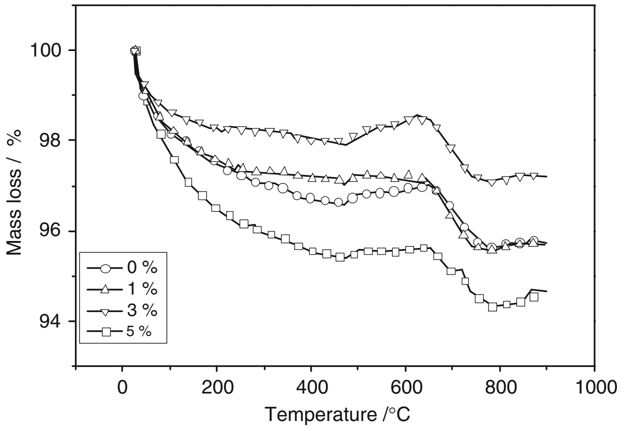

Fig. 1 TG curves of BG with different amounts of Ag. The samples were previously treated at 600 °C/4 h

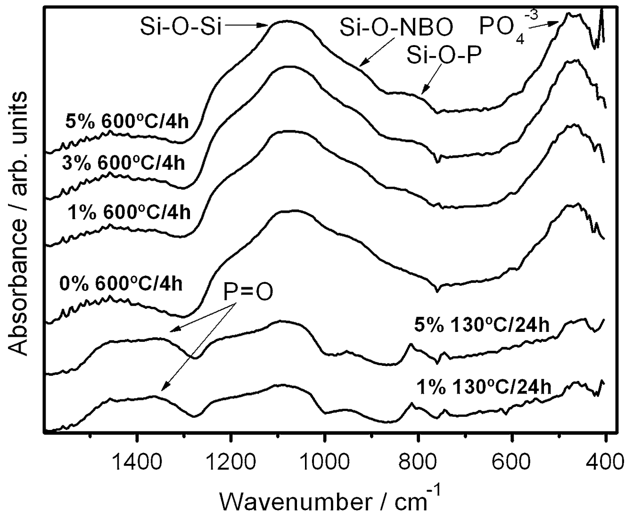

Fig. 2 FTIR absorption of BG for the samples dried at 130 °C and the ones further treated at 600 °C

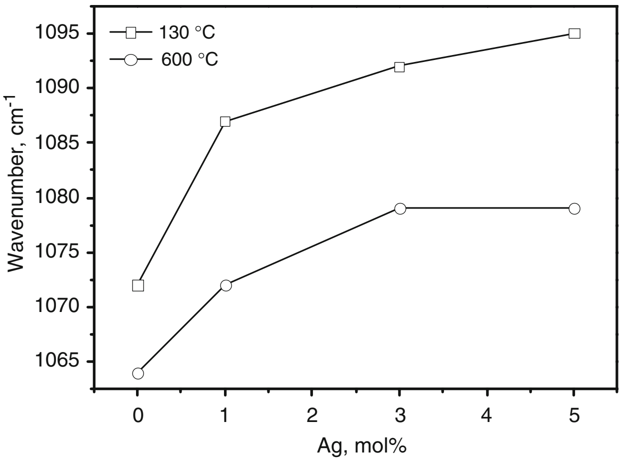

Fig. 3 Infrared absorption peak position of BG containing silver

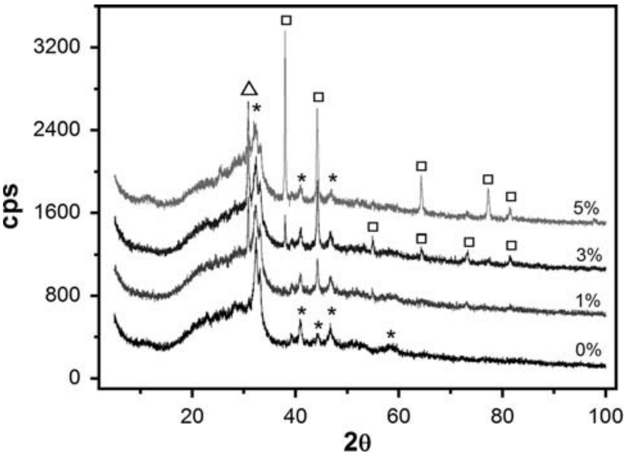

Fig. 4 DRX pattern of BG with different amounts of silver (*open triangle*), SiO$_2$ (*open square*), and Silver (*asterisk*) HA

are due to the adsorbed water and increase as the amount of silver in the samples is decreased. In this class of bioactive glasses, water affinity is proportional to the non-bridging oxygen, which is related to the amount of Si–O–NBO on the BG surface [18]. Therefore, we can assume that the Si–O–NBO bonding number is being reduced by silver.

Modifier elements cause the occurrence of non-bridging oxygen (NBO) and discontinuity in the vitreous network; but silver has an opposite effect in these samples. In FTIR curves (Fig. 2), we can identify the main vibrational modes: (i) Si–O–Si stretching at 1,000–1,200 cm^{-1}, (ii) Si–O–NBO stretching at 890–975 cm^{-1}, (iii) Si–O–Si bending near 750 cm^{-1}, and (iv) PO$_4^{-3}$ antisymmetric bending at 570–600 cm^{-1}, associated with phosphorous in a crystal-like environment [17]. For the samples treated at 600 °C, the bands at 1,000–1,200 cm^{-1} and 500 cm^{-1} have higher intensities and widths due to the densification of the vitreous structure with increasing numbers of these bond sites, compared to the peaks of the samples that are only dried at 130 °C. The crystal-like site formation and structure densification is evidenced by the increase of the PO$_4^{-3}$ band [19].

In contrast, a higher concentration of modifiers in the glasses leads to a higher degree of depolymerization in the structure and a higher concentration of the Si–O–NBO groups. These functional groups control the dissolution of the silica through the formation of silanol in SBF. The samples containing 3% and 5% silver exhibited greater increases in the bands attributed to bridging oxygen (BO) and to phosphate. This fact can cause a solubility reduction of BG in SBF, explaining the hygroscopic decrease of BG with higher silver content.

The bond energy of Si–O–Si decreases considerably with the thermal treatment and increases with an increasing amount of silver (Fig. 3). The thermal treatment causes structure densification by eliminating carbon compounds, thereby reducing the mean bond energy. The silver addition modifies the BG structure, increasing its density by reducing the amount of Si–O–NBO.

The X-ray diffractograms (Fig. 4) of the samples containing silver exhibited mainly amorphous characteristics corresponding to glass, but they showed incipient crystallization of quartz, metallic silver and hydroxyapatite.

An increase in the amount of silver caused an increase of quartz and metallic silver crystallization while reducing hydroxyapatite crystallization. Therefore, silver could be released in the biological organism after BG implantation as ions or as metallic silver particles.

The mean particle size of BG was under 100 nm (Fig. 5). The particles were partially agglomerated.

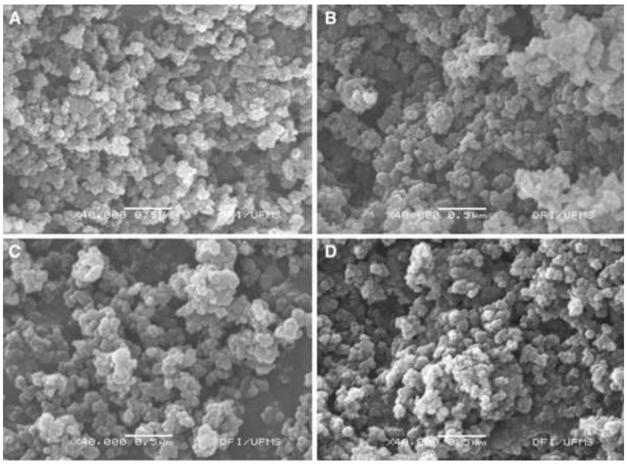

Fig. 5 VBA heat-treated at 600 °C with (**a**) 0%, (**b**) 1%, (**c**) 3%, and (**d**) 5% of Ag content

Conclusions

The mass losses of BG attributed to free and surface water occurred at 70 and 150 °C, and the decomposition of organics occurred near 510 and 650 °C. The water loss is greater at lower silver concentrations, and the bioactive glass can stabilize around 510 °C. When stabilization occurred, FTIR showed that the organics were partially eliminated, and there was an increase in the absorption peaks associated with Si–O–Si bonds, revealing densification of the vitreous matrix. The intensities of these peaks increased with silver content. Therefore, since silver improves the Si–O–Si bond number, it contributed to densification, explaining how hygroscopy decreases with increasing silver concentration. In the XRD patterns, we observed that the samples with no silver crystallized mainly as hydroxyapatite, while the samples containing 3 and 5% silver crystallized the hydroxyapatite, silica and silver metallic phases. We obtained BG nanometer-sized particles for all the samples. The silver reduction has previously been reported for silica glasses. We observed the silver reduction resulting in metallic silver for bioactive glasses containing a minimum of 3% silver.

Acknowledgements This work has been supported by FINEP, CNPq, FUNDECT, and by UFMS.

References

1. Costa HS, Rocha MF, Andrade GI, Barbosa-Stancioli EF, Pereira MM, Orefice RL, et al. Sol-gel derived composite from bioactive glass-polyvinyl alcohol. J Mater Sci Mater Med. 2008;43:494–502.
2. Hench LLJ. The story of Bioglass®. Mater Sci Mater Med. 2006;17:967–78.
3. Chatzistavrou X, Zorba T, Chrissafis K, Kaimakami G, Kontonasaki E, Koidis P, et al. Influence of particle size on the crystallization process and the bioactive behavior of a bioactive glass system. J Therm Anal Cal. 2006;85:253–9.
4. Du RL, Chang J, Ni SY, Zhai WY. Characterization and in vitro bioactivity of zinc-containing bioactive glass and glass-ceramics. J Biomater Appl. 2006;20:341–60.
5. Aina V, Perardi A, Bergandi L, Malavasi G, Menabue L, Morterra C, et al. Cytotoxicity of zinc-containing bioactive glasses in contact with human osteoblasts. Chemico-Biol Interact. 2007;167:207–18.
6. Monem AS, Elbatal HA, Khalil EMA, Azooz MA, Hamdy YM. In vivo behavior of bioactive phosphate glass-ceramics from the system P2O5–Na2O–CaO containing TiO_2. J Mater Sci Mater Med. 2008;19:1097–108.
7. James PF. Glass ceramic: new compositions and uses. J Non-Cryst Solids. 1995;181:1–15.
8. Navarro M, Ginebra MP, Clement J, Salvador M, Gloria A, Planell JA. Physicochemical degradation of titania-stabilized soluble phosphate glasses for medical applications. J Am Ceram Soc. 2003;86:1345–52.
9. Balamurugan A, Balossier G, Michel J, Kannan S, Benhayoune H, Rebelo AHS, et al. Sol gel derived SiO_2–CaO–MgO–P_2O_5 bioglass system-preparation and in vitro characterization. J Biomed Mater Res B. 2007;83:546–53.
10. Efflandt SE, Magne P, Douglas WH, Francis LF. Interaction between bioactive glasses and human dentin. J Mater Sci Mater Med. 2002;13:557–65.
11. Ning J, Yao A, Wang D, Huang W, Fu H, Liu X, et al. Synthesis and in vitro bioactivity of a borate-based bioglass. Mater Lett. 2007;61:5223–6.
12. Marion NW, Liang W, Reilly G, Day DE, Rahaman MN, Mao JJ. Borate glass supports the in vitro osteogenic differentiation of human mesenchymal stem cells. Mech Adv Mater Struct. 2005;12:239–46.
13. Huang W, Day DE, Kittiratanapiboon K, Rahaman MN. Kinetics and mechanisms of the conversion of silicate (45S5), borate, and borosilicate glasses to hydroxyapatite in dilute phosphate solutions. J Mater Sci Mater Med. 2006;17:583–96.
14. Munukka E, Leppäranta O, Korkeamäki M, Vaahtio M, Peltola T, Zhang D, et al. Bactericidal effects of bioactive glasses on clinically important aerobic bacteria. J Mater Sci Mater Med. 2008;19:1927–32.
15. Bellantone M, Coleman NJ, Hench LL. Bacteriostatic action of a novel four-component bioactive glass. J Biomed Mater Res. 2000;51:484–90.
16. Clupper DC, Hench LL. Bioactive response of Ag-doped tape cast Bioglass® 45S5 following heat treatment. J Mater Sci Mater Med. 2001;12:917–21.
17. Carta D, Knowles JC, Smith ME. Synthesis and structural characterization of P_2O_5–CaO–Na_2O sol–gel materials. J Non-Cryst Solids. 2007;352:1141–9.
18. Aguiara H, Solla EL, Serra J, González P, León B, Almeida N, et al. Orthophosphate nanostructures in SiO_2–P_2O_5–CaO–Na_2O–MgO bioactive glasses. J Non-Cryst Solids. 2008;354:4075–80.
19. Cieciñska M. Thermal analysis of gel-derived bioactive phosphosilicate glasses. J Therm Anal Cal. 2003;72:199–207.